Effect of Specimen Geometry on Fatigue Crack Propagation in Threshold Region

P. Hutař[1], S. Seitl[1], T. Kruml[1]
[1]*Institute of Physics of Materials of the Academy of Sciences of the Czech Republic, v. v. i., Brno Czech Republic*

1 Introduction

Over the years, a number of relationships have been developed to represent the whole typical range of fatigue crack growth rate (FCGR) data or at least some parts of it. The simplest of these is the Paris equation [1] developed in 1963 to represent the linear region of the fatigue crack growth curve (the dependence of FCGR on range of the stress intensity factor (SIF)):

$$\frac{da}{dN} = C(\Delta K)^m \tag{1}$$

where ΔK is the range of the stress intensity factor. C and m are empirical parameters determined from a curve fit to test data. In our case loading cycle stress ratios are close to R=0, therefore $\Delta K = K_I = K_{max}$. This original model is still in use today for many applications; more advanced models essentially broaden Paris equation validity by addressing mean stress effects, threshold behavior or fatigue crack closure effects.
The aim of this paper is to provide a description and analysis of experimental results involving geometry effects observed between the C(T) and M(T) specimens in two different steels. The authors will present their own laboratory fatigue crack growth rate test data measured on two different specimens with different levels of constraint. The constraint level can be described in the framework of linear elastic fracture mechanics by the second term of Williams expansion, T-stress. The magnitude of the T-stress affects the size and shape of the plastic zone and can influence the behaviour of the fatigue crack. It is demonstrated that fatigue characteristics (i.e. C, m and ΔK_{th}) obtained from measurement using different specimen geometries are not only properties of the material, but also depend on the constraint level.

2 Experimental results

The materials used in this investigation were the EUROFER 97 steel and the low carbon steel 15313, see Table 1. The material properties corresponding to the EUROFER 97 are Young's modulus E=2.1×10^5 MPa, Poisson ratio ν =0.3, cyclic yield stress σ_0 = 400 MPa.
For the low carbon steel 15313, following material characteristics were estimated: Young's modulus E=2.0×10^5 MPa, Poisson ratio ν =0.3, cyclic yield stress σ_0 = 330 MPa.

[1] E-mail adress : hutar@ipm.cz , seitl@ipm.cz , kruml@ipm.cz

Table 1. Steels chemical composition (wt %)

	C	Mn	Si	P	S	Cr	Ni	Mo	V	Ta
Eurofer 97	0.10	0.54	0.025	0.0025	0.001	9.06	0.013	0.005	0.225	0.115
15313	0.10	0.60	0.40	0.035	0.035	2.3	0.60	1.05	0	0

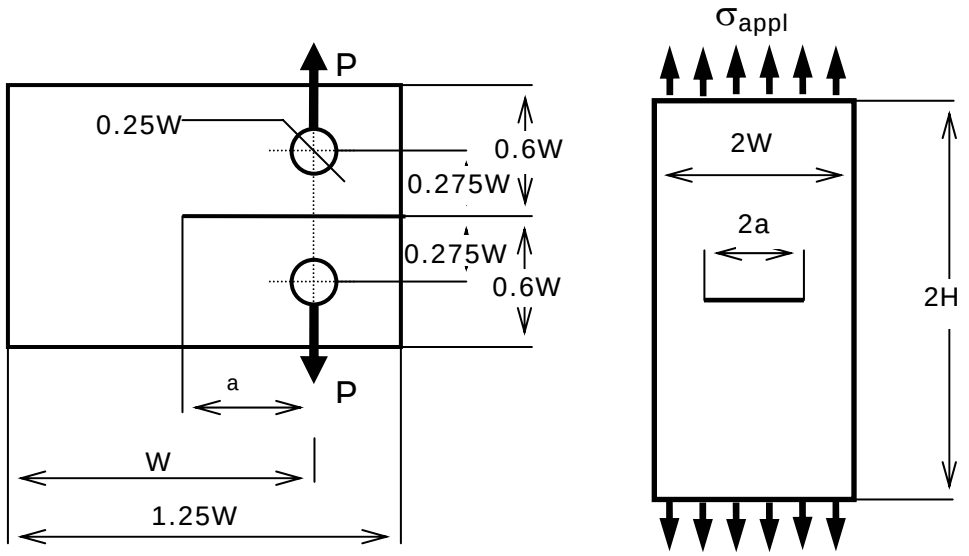

Fig. 1. Schematic of C(T) and M(T) specimen geometries. (W=50, H=150 and thickness =10; dimensions in mm). $a/W \in (0.3; 0.7)$.

Fatigue crack growth rate tests following the ASTM standard [2] were performed for both materials on two geometrically different specimens: C(T) Standard Compact-Tension Specimen and M(T) Standard Middle-Tension Specimen, see Fig.1. Experimental tests were operated at room temperature with stress ratio R=0.1. The tests were conducted employing computer controlled high-frequency resonating machines. Threshold conditions are achieved for long fatigue cracks by K decreasing test by stepped shedding, ΔK, as the crack propagates. The fatigue crack threshold is reached when the crack stops growing. Because the load reduction occurs gradually as the crack grows, no true threshold is reached in a practical amount of time. Instead, a working definition for ΔK_{th} is used as very low FCGR are achieved (10^{-10} m/cycle has been suggested) [2]. Frequencies in the threshold region were in the range of 60 Hz to 90 Hz, which had no influence on fatigue crack behavior. Crack length was monitored using an optical microscope marked in increments of 0.01 mm.

Fig. 2. shows the fatigue crack propagation property of the tested EUROFER 97 steel plate which was obtained using standard C(T) and M((T) specimens. There is not a significant difference in the crack growth behaviour between the two specimen geometries except in the lowest part of crack growth rate. This is in agreement with our previous experimental study [3]. Over this range, the M(T) specimen showed slightly lower fatigue crack growth rates and a lower threshold then the C(T) specimen. Similarly, for the 15 313 steel, there is no significant

difference in crack growth behaviour between two specimen geometries for FCGR for ΔK higher than 10 MPa $m^{1/2}$. For both materials, the threshold values are really geometry sensitive. The stress ratio is R=0.1, therefore FCGR close to the threshold can be influenced by fatigue crack closure effects. The large shift of the threshold observed for the C(T) specimen may be the result of the significantly higher crack opening loads in comparison to those for the M(T) specimen.

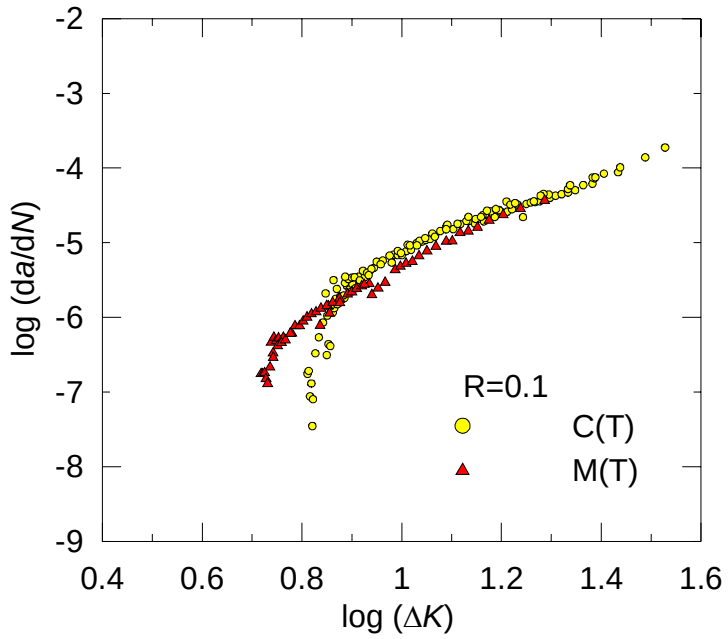

Fig. 2. The FCGR versus the stress intensity factor (SIF) range for the EUROFER 97, R=0.1

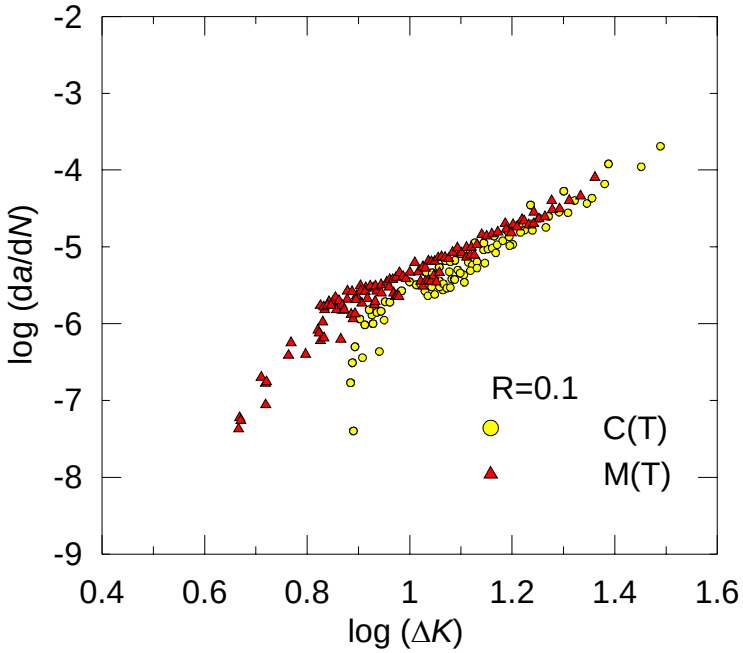

Fig. 3. The FCGR versus the SIF for the 15313 steel, R=0.1

Table 2. The threshold values of SIF and *C, m* scaling constants of Paris law.

Steel	*R*	Specimen	ΔK_{th} [MPa m$^{1/2}$]	*C*	*m*
EUROFER 97	0.1	C(T)	6.50	4.00×10^{-8}	2.36
		M(T)	5.25	1.00×10^{-9}	3.54
15313	0.1	C(T)	7.70	1.60×10^{-10}	4.06
		M(T)	4.50	2.11×10^{-9}	3.28

3 Crack closure

Crack closure has been accepted as an important phenomenon in fatigue crack propagation. For accurate prediction of the fatigue life and also the interpretation of the FCGR in different structures, it is necessary to evaluate the crack tip opening values exactly. In our case, mainly the effect of the plasticity induced crack closure and roughness induced crack closure can be considered as present. The roughness-induced crack closure is attributed to crack path deflection, especially at relatively low crack growth rates [4]. On the other hand, plasticity induced crack closure is dominant over a broad range of stress intensity factors. Generally, the closure effects are implemented in the Paris equation using the following formula:

$$\frac{da}{dN} = C(K_{\max} - K_{op})^m \tag{2}$$

where K_{max} is the maximal stress intensity factor (corresponding to ΔK in our case) and K_{op} is the stress intensity factor corresponding to the crack opening values.

3.1 Plasticity induced crack closure

The phenomenon of plasticity induced crack closure was first investigated by Elber. During cyclic loading, large tensile plastic strains are developed near the crack tip, which are not fully reversed upon unloading. This leads to the formation of the plastic wake behind the crack tip as the crack extends, and a subsequent reduction of the driving force for fatigue crack growth. A number of researchers have attempted modeling plasticity induced crack closure using the finite element method (FEM) [5, 6].

In our case, the two different specimens used for experimental observation were modeled using finite elements to predict plasticity induced crack closure, see Fig.4.

The cyclic behavior of low carbon steels in the numerical calculations has been characterized by the Chaboche material model [6]. The Chaboche model can be described by this equation:

$$dX = B\left(\frac{2}{3}A.d\varepsilon_p - X.dp\right), \tag{3}$$

where B and A are material parameters of the model, ε_p is a plastic deformation tensor, p is the accumulated equivalent plastic strain and X is the kinematic part of the stress tensor. This equation describes the non-linear behavior of material with kinematic stress hardening. Eq.3 is used if $J_2(S-X)=R_o$, in the other case the material behavior is purely elastic. J_2 is the second invariant of deviatoric stresses, S is a stress tensor and R_0 is the elastic limit. The parameters of the Chaboche model were deduced from the nonlinear part of the cyclic stress-strain curve. The final values of the Chaboche parameters corresponding to steel 15313 used for our numerical calculations were: R_0=280 MPa, A=220 MPa and B=500.

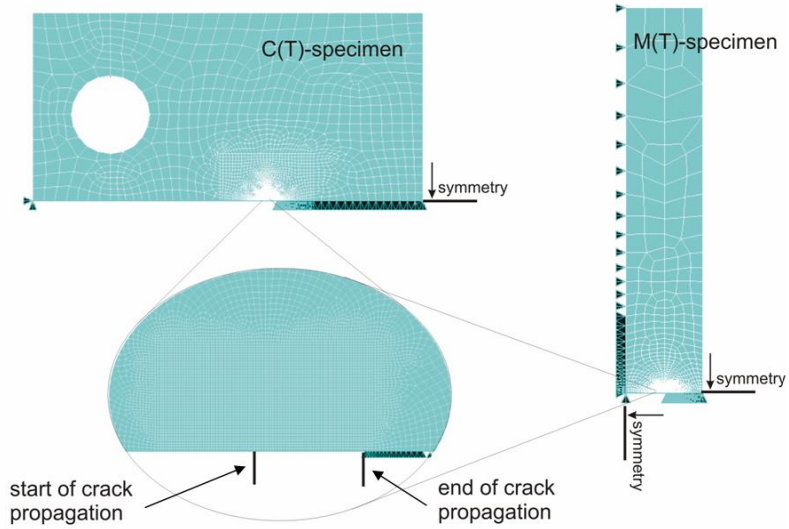

Fig. 4. Model of M(T) and C(T) specimen used for elasto-plastic FEM computations

The model presented (Fig.4.) was cyclically loaded with the constant amplitude of the stress intensity factor corresponding to the experimental conditions. Ten full cycles were applied with stress ratio R=0. Symmetric finite element models typically contain 10,000 of eight-node isoparametric elements. Further mesh refinements have no influence on calculated results.

The effect of the applied loading level (expressed by K_{max}) on the plasticity induced crack closure is shown in Fig.5. In the area where small scale yielding conditions are valid, the ratio between the opening stress intensity factor (K_{op}) and K_{max} is rather constant. For higher applied loading this ratio slowly decreases, which is in agreement with results published by Solanki et al. [5].

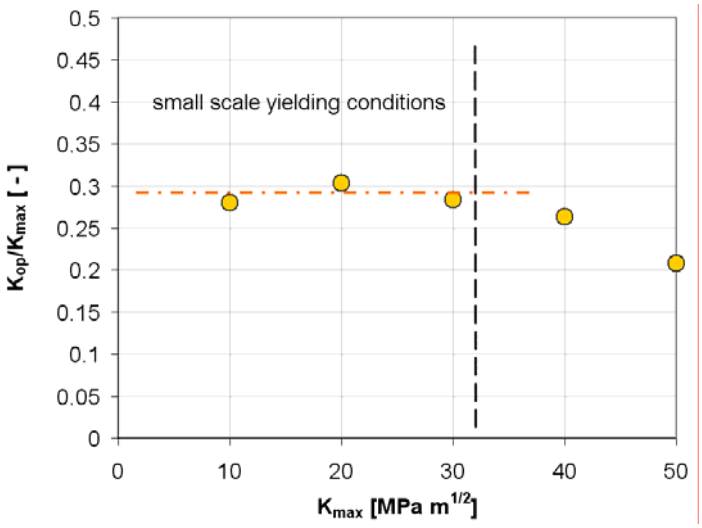

Fig. 5. Typical dependence of the plasticity induced crack closure on applied load level. Model of M(T) specimen and R=0 are used

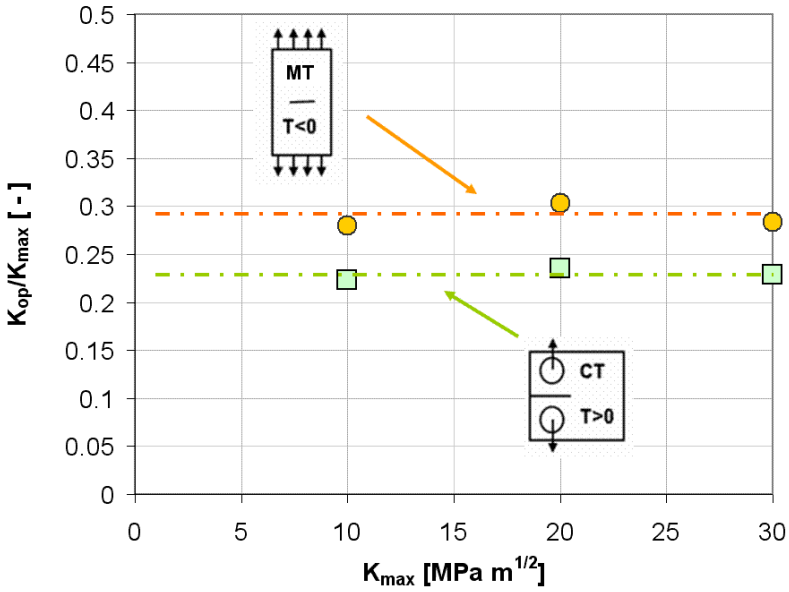

Fig. 6. Comparison of the plasticity induced closure levels between M(T) and C(T) specimens

A comparison between plasticity induced crack closure level for M(T) specimen with C(T) one is presented in Fig. 6. Difference between levels of plasticity induced crack closure for these two geometries is about 6 % of the maximal stress intensity factor. Higher closure level for M(T) specimen means lower FCGR, which is in contradiction with experimental results especially in threshold area. It can explain the small decrease in the FCGR obtained for M(T) specimen for higher ΔK values visible only on the results obtained for EUROFER 97 steel. Close to the threshold, the effect of the plasticity induced crack closure is thus shielded by different phenomena.

3.2 Roughness induced crack closure

Many experimental data showed the concurrence of the roughness-induced crack closure and plasticity induced crack closure [8]. Usually these crack closure effects are difficult to separate by experimental methods. Nevertheless, close to the threshold, roughness induced crack closure can be dominant. For the near-threshold tests, the fracture surfaces became more crystallographic in nature and more sensitive for local grain disorientation. In those cases, the plastic zone size is comparable with microstructural unit of the material, see Fig. 7. The typical size of the plastic zone in plain strain conditions can be easily computed using the equation:

$$r_y(\theta) = \frac{1}{4\pi}\left(\frac{K_{\max}}{\sigma_0}\right)^2\left[(1-2\nu)^2(1+\cos\theta)+\frac{3}{2}\sin^2\theta\right] \qquad (4)$$

where σ_0 is the cyclic yield stress of material. The Eq.(4) defines the approximate boundary between elastic and plastic behaviour.

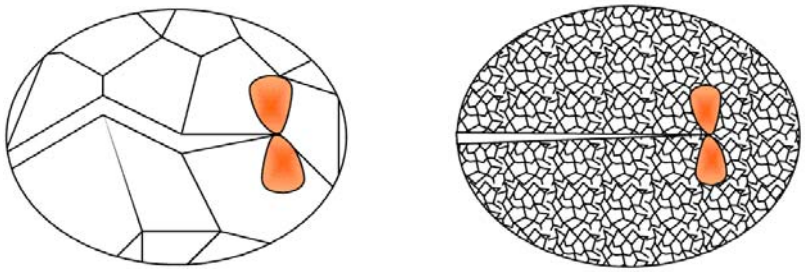

Fig. 7. Comparison of the plastic zone size with typical microstructural unit for threshold loading level and high loading level.

For the EUROFER 97 steel in the threshold area, the plastic zone size is about 12 μm and the mean size of prior austenitic grain is reported to be around 15 μm. Using electron backscatter diffraction (EBSD) technique dimensions of the blocks with same crystallographic orientation were determined (see Fig. 8.). It can be seen that most of blocks are of about 5 μm in diameter but at least two much larger blocks are present in the observed region: the brown area at the top of the right figure and the blue-green area at the left bottom. It proves that some blocks larger than 20 μm are present.

It can be concluded that for threshold crack growth rates the plastic zone size is comparable with the microstructural unit of the material. Therefore, fracture surface roughness could increase as the K_{max} level decreases. This conclusion is in agreement with the observations of Linkes and Stephens [9]. A rougher fracture surface leads to a greater effect of mode II during fatigue crack growth, and could lead to higher crack opening loads. Geometry with low constraint level (M(T) specimen) produces a much bigger plastic zone near the crack tip than geometry with a high level of the constraint (C(T) specimen) [10]. It can thus be assumed that for $\Delta K \sim 8$ MPa $m^{1/2}$, where the C(T) and M(T) specimens start to show different FCGR behaviour (Fig. 2.), the plastic zone size in C(T) specimens

reaches a comparable dimension with the largest block size. In addition, the stress distribution around the crack tip is changed due to different biaxiality. It is known that a low level of the constraint leads to better stabilization of the crack in mode I during crack propagation [11]. It can lead to higher fracture surface roughness for C(T) specimen and consequently to higher level of roughness induced crack closure. These phenomena can at least partially explain differences between threshold values obtained for the C(T) specimen and the M(T) specimen.

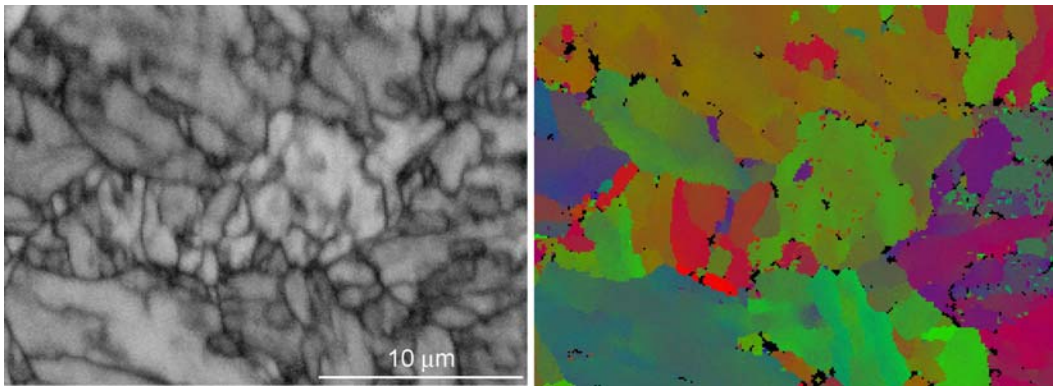

Fig. 8. As-received microstructure of the EUROFER 97 steel in EBSD imaging. Left: quality pattern of the EBSD procedure. Dark lines follow the grain boundaries. Right: the same area artificially coloured according to the crystallographic direction of the normal to the specimen surface. Areas with similar colour also display a similar crystallographic orientation.

4 Conclusions

The effect of constraint on the propagation of the fatigue crack was studied both theoretically and experimentally. Due to the strong difference in fatigue crack propagation rates in the threshold region obtained for C(T) and M(T) specimens for two different low carbon steels, it is not appropriate to use a fitting of all experimental data by the same material curve, which is independent of the outer geometry of the specimen, as is usually presented in the literature [12]. The level of constraint induced by the different geometry of the specimen has to be considered. Fatigue crack growth close to the threshold is usually influenced by crack closure effects. With the decreasing of the ΔK values the size of the cyclic plastic zone also decreases and becomes comparable with the microstructural units of the material. For this reason, in the threshold region fatigue crack growth is microstructure sensitive and roughness induced by crack closure induced by fracture surface roughness occurs. A different constraint level can influence the intensity of the crack closure. Experimental measurements [9] of the crack closure effect for different levels of the stress intensity factor range confirm this idea and indicate a much larger closure effect in the threshold area for specimens with a high level of the constraint (C(T)) than for specimens with a low level of the constraint (M(T)). Therefore, the transferability of experimentally obtained threshold values between different specimens is only possible assuming the same

constraint level. For a conservative estimation of the residual fatigue life time of the structures it is better to use specimens with low level of the constraint. A deeper understanding of the mechanism of the fatigue crack propagation in the threshold region in order to prevent unexpected failure of the structural components is of paramount importance for damage tolerant design applications.

Acknowledgments

This investigation was supported by projects nos. 101/08/1623, 101/09/0867 and 106/09/1954 of the Czech Science Foundation.

References

[1] Paris, P. and Erdogan, F. A critical analysis of crack propagation laws, Journal of Basic Engineering, Transactions of the American Society of Mechanical Engineers (1963) 528-534.

[2] ASTM Standard E647-00, Standard Method for Measurement of Fatigue Crack Growth Rates, ASTM 03.01, (2004)

[3] Seitl, S. Hutař, P., Knésl, Z. Sensitivity of fatigue crack growth data to specimen geometry, Key Engineering Materials Vols. 385-387 (2008) 557-560

[4] Ritchie, R.O., Suresh, S., Some considerations on fatigue crack closure at near-threshold stress intensities due to fracture surface morphology, Metal Trans Vol. 13A (1981) 937-940

[5] Solanki K., Daniewicz, S.R., Newman, J.C. Finite element analysis of plasticity-induced fatigue crack closure: an overview, Engineering Fracture Mechanics 71 (2004) 149-171

[6] Lopez-Crespo, P. Camas-Pena, D., Gonzalez-Herrera, A., Yates, J.R., Patterson, E.A., Zapatero, J. Numerical and experimental analysis of crack closure, Key Engineering Materials Vols. 385-387 (2008) 369-372

[7] Lemaitre J., Chaboche J.L., Mechanics of Solid Materials, Springer-Verlag, (1987)

[8] Kim C.Y., Song J.H., Fatigue crack closure and growth behavior under random loading, Engng. Fract. Mech Vol. 49 (1994) 105-120

[9] Linkes H. O., Stephens R.R., Effect of geometry and load history on fatigue crack growth in Ti-62222, Fatigue crack growth thresholds, endurance limits, and design, ASTM STP 1372, (2000)

[10] Anderson T.L., Fracture Mechanics, CRC Press, Boca Raton, Florida, (1995).

[11] Pook LP. Linear Elastic Fracture Mechanics for Engineers: Theory and Applications. WIT Press, (2000).

[12] Klesnil M., Lukáš P., Fatigue of Metallic Materials, Elsevier, Amstredam, (1992)